

Proceedings of the Research Institute of Atmospherics,  
Nagoya University, vol. 26 (1979)

## THE EFFECT OF THE EARTH-IONOSPHERE WAVEGUIDE PROPAGATION ON THE POLARIZATION AND ARRIVAL ANGLES OF WHISTLERS

Shin-Ichi MORIYAMA, Toshimi OKADA, Masashi HAYAKAWA  
and Akira IWAI

### Abstract

The purpose of the present paper is to discuss the effect of the Earth-ionosphere waveguide propagation on the polarization and arrival angles of whistlers for a refined model of calculation. It is found that the effect of multi-rays is, generally, relatively small for incident angles less than  $60^\circ$  for which the field analysis direction finding is very effective, but it is very large for higher incident angles. This effect appears as the error in arriving direction less than  $15^\circ$  for nighttime and  $10^\circ$  for daytime for incident angles less than  $60^\circ$ . The azimuthal dependence of the effect of multi-rays is first studied, and it shows slight dependence in which the effect is maximized in the North to South propagation in the Northern hemisphere. The resultant polarization does not differ from the limiting polarization for a direct ray and it is nearly circular. These theoretical calculations are compared with experimental data, resulting in a necessity of the refinement of the model of wave emergence at the base of the ionosphere.

### 1. Introduction

The direction finding (DF) to locate the ionospheric exit points

of whistlers is of current importance in the study of the propagation characteristics of whistlers in the magnetosphere and of magnetospheric plasma (Cousins, 1972; Bullough and Sagredo, 1973; Rycroft et al., 1974; Tsuruda and Hayashi, 1975; Okada et al., 1977; Leavitt et al., 1978). A comparison of the DF data with the conventional dispersion analysis has yielded one of the most important recent discoveries that the field-aligned whistler ducts do not extend down to the  $F_2$  region but normally terminate at the base of the protonosphere, say above 1000 km (Rycroft et al., 1974; Corcuff, 1975). In interpreting the data obtained by the field analysis direction findings (Tanaka, 1972; Tsuruda and Hayashi, 1975; Tanaka et al., 1976; Okada et al., 1977; Leavitt et al., 1978) the most serious point to consider is the effect of multi-rays propagating in the Earth-ionosphere waveguide on the measurement of the incident and azimuthal angles and the polarization of whistlers, which is the subject of the present paper. Namely the effect is thought to appear as the polarization error in the DF measurement. Crary (1961) made a detailed study on the influence of multi-rays on the DF accuracy, but he has dealt with a simple model such as a sharply bounded ionosphere and QL approximation for the wave refractive index of the ionosphere, which are quite insufficient when comparing with our observed characteristics of arrival angles and the polarization. His QL approximation prevented him from studying the azimuthal variation of polarization error due to the presence of the Earth's magnetic field, which is first investigated in this paper. We follow approximately the line of Crary (1961) to estimate the effect of the Earth-ionosphere waveguide propagation on the accuracy of the DF and polarization, but we made a few essential improvements including the inhomogeneity of the lower ionospheric model and the Earth's magnetic field. These theoretical calculations are compared with experimental data.

Inclusion of the ionospheric inhomogeneity will make us to use the full-wave method to calculate the ionospheric reflection and transmission coefficients, which are essentially important in this paper and so described briefly in Section 2. Then in Section 3 we present the process of our calculation, and the computational results of the resultant polarization and DF accuracy are given in Section 4. Finally in Section 5 we compare the theoretical polarization with previous measurements, and point out the future work to be done.

## 2. Full-wave calculation of the ionospheric reflection and transmission coefficients

### 2.1. Calculation of reflection coefficients of upgoing waves

The wave equation governing the propagation of waves in a horizontally stratified ionosphere is given by (Pitteway, 1965)

$$\vec{d}\vec{e}/dz = -jk_0 \hat{T} \vec{e} \quad (1)$$

$$\vec{e} \equiv (E_x, E_y, -Z_0 H_x, Z_0 H_y) \quad (\text{column vector})$$

where  $k_0$  is the free space wave number,  $Z_0$  the characteristic impedance of free space and  $\hat{T}$  is a matrix determined by the propagation parameters (see Pitteway, 1965).

Eq. (1) is numerically integrated downward with the eigen vectors at a sufficient height as the initial values and then the two solutions for the wave incident on to the ionosphere from below are given; the penetrating mode solution  $\vec{e}_2$  and the non-penetrating mode solution  $\vec{e}_1$ . The transmission coefficient for the penetrating mode solution is given by (Pitteway and Jespersen, 1966)

$$T = \sqrt{\frac{1}{n} R_e (E_x Z_0 H_y^* - E_y Z_0 H_x^*)} \quad (2)$$

where  $\ell$ ,  $m$  and  $n$  are the direction cosines of the wave normal for a plane wave incident on the ionosphere from below and  $R_e$  denotes the real part of the quantity.

In free space below the ionosphere, each wave-field variable can be resolved into an upgoing (incident) part  $U$  and a downgoing (reflected) part  $D$ ;  $\vec{e}_1 = \vec{U}_1 + \vec{D}_1$ ,  $\vec{e}_2 = \vec{U}_2 + \vec{D}_2$ . The reflection coefficients  ${}_{\parallel}R_{\parallel}$ ,  ${}_{\parallel}R_{\perp}$ ,  ${}_{\perp}R_{\perp}$  and  ${}_{\perp}R_{\parallel}$  of the ionosphere are conveniently described by the components of Pitteway (1965) in the following way

$$\begin{aligned} \begin{pmatrix} {}_{\perp}R_{\perp} & -{}_{\perp}R_{\parallel} \\ {}_{\parallel}R_{\perp} & -{}_{\parallel}R_{\parallel} \end{pmatrix} &= (1/nW) \begin{pmatrix} C & S \\ -nS & nC \end{pmatrix} \begin{pmatrix} -U_{y,2} & U_{y,1} \\ -U_{x,2} & U_{x,1} \end{pmatrix} \\ &\times \begin{pmatrix} D_{x,1} & -D_{y,1} \\ D_{x,2} & -D_{y,2} \end{pmatrix} \begin{pmatrix} nC & -S \\ nS & C \end{pmatrix} \end{aligned} \quad (3)$$

where  $S = \sin\theta$ ,  $C = \cos\theta$ ,  $W = -U_{x,1}U_{y,2} + U_{y,1}U_{x,2}$  and  $\theta$  is the azimuthal angle relative to the magnetic North.

The polarization ellipse is defined by projection from above on to the ground plane, using two convenient angular parameters  $\phi$  and  $\psi$  such that

$$\tan\phi = |U_y/U_x| , \quad \psi = \arg(U_y/U_x) \quad (4)$$

## 2.2. Transmission coefficient of downgoing whistler waves

The transmission coefficient and polarization for downgoing whistler waves can be deduced from those for upgoing waves by means of a reciprocity theorem (Pitteway and Jespersen, 1966). The penetrating mode incident with an angle of incidence  $I$  and azimuth  $\theta$  is reciprocal with the downgoing whistler, emerging at an angle  $I$  from the vertical in an azimuthal direction  $(180^\circ - \theta)$ . When the penetrating mode solution has azimuth angle  $\theta_1$ , chosen to the azimuth for the downgoing whistler  $\theta_2$  so that  $\theta_1 + \theta_2 = 180^\circ$ , the transmission coefficients are the same and the one polarization is obtained from the other by taking  $\phi$  the same and replacing  $\psi$  by  $(180^\circ - \psi)$ .

To study the characteristics of the limiting polarization, we use the polarization  $Q$  defined in the plane perpendicular to the emerging wave normal. For polarization at azimuthal angle  $\theta$  the polarization  $Q$  is related to the polarization parameters  $\phi$  and  $\psi$  by

$$Q = \cos I \cdot \frac{\tan\phi \cdot \exp(j\psi) \cdot \sin\theta - \cos\theta}{\tan\phi \cdot \exp(j\psi) \cdot \cos\theta + \sin\theta} \quad (5)$$

## 3. The effect of the earth-ionosphere waveguide propagation on whistlers

We follow Crary's (1961) line to calculate the effect of multi-rays on the physical parameters of whistlers. First we make a few assumptions to simplify the computations.

1. Each individual ray component can be treated as a plane wave in the antenna area, and the antenna is considered to be in the far field.

2. All the energy in a set of sky-wave components is assumed to be of the same frequency, although, actually, various rays contributing

to a whistler signal at a given time are of slightly different frequency because of the frequency variation of the whistler and the difference in propagation times of the rays.

3. Although we consider the inhomogeneity of the ionosphere, being essentially different from previous works, the lowest boundary is assumed to be terminated at a specific height ( $h_r$ ) which contributes to the partial reflection most efficiently, and is given by (Hayakawa and Shimakura, 1978)

$$h_r = \frac{1}{\gamma} \cdot \ln \frac{\omega}{\omega_r(0)} \quad (6)$$

where  $\omega_r(z) = \omega_r(0) \cdot \exp(\gamma z)$  ( $= \omega_p^2 / \nu$ :  $\omega_p$ , electron plasma frequency,  $\nu$ , electron collision frequency) and the lower part of the profile can be approximated by being exponential (see Fig.3).  $\omega_r(0)$  is the value attained on the ground. The height ( $h_r$ ) is assumed to be same for all sky-wave components. This termination is confirmed to have a negligible influence.

4. The plane wave energy is assumed to be uniform within the transmission cone in the ionosphere. Then it is assumed that the transmitted waves may be considered to radiate from a point source.

Next we have to formulate a system of equations for calculating the total field for the whistler-mode signal which arrives at a receiving antenna. The ray geometry is illustrated in Fig.1.

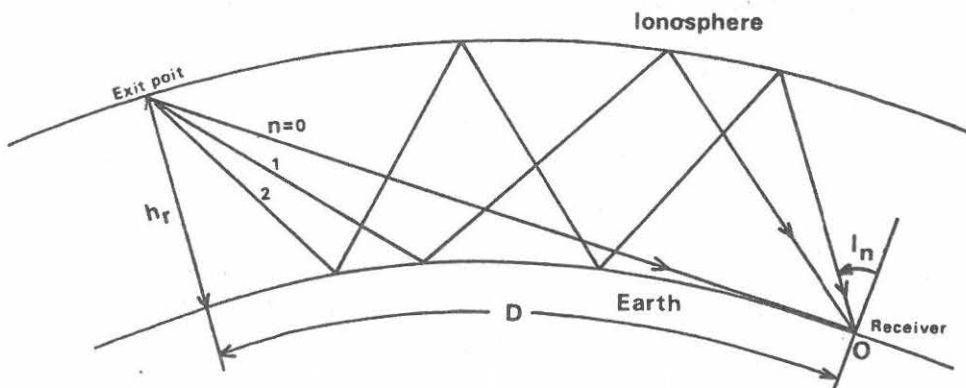


Fig.1 Ray geometry for multi-rays with  $n=0,1$  and  $2$ . The Earth is a perfect sphere of radius  $6367.39\text{km}$ . The angle  $I_n$  is determined by the reflection height  $h_r$ , the ground distance  $D$  to the receiver and the number of ionospheric reflections  $n$ .

The expression for the transmitted waves below the ionosphere may be written by using the transmission coefficient  $T$  and limiting polarization  $Q$  described in Section 2.2.

$$E_{\parallel t} = T/\sqrt{1+|Q|^2} \quad (7)$$

$$E_{\perp t} = T \cdot |Q| \cdot \exp[j \cdot \arg(Q)] / \sqrt{1+|Q|^2} \quad (8)$$

The subscripts  $\parallel$  and  $\perp$  indicate that the electric field is parallel to or perpendicular to the plane of incidence, respectively.

The transmitted wave given by Eqs.(7) and (8) is then reflected  $n$  times by the Earth and ionosphere before arriving at the receiver. The reflections from the ionosphere are described by the four reflection coefficients (Eq.(3)), while the reflections from the Earth are expressed in terms of the Fresnel reflection coefficients  $R_{\parallel}$  and  $R_{\perp}$ . The electric field for each ray is calculated as the sum of  $n$  sky-wave components by using these six reflection coefficients. The addition of components can be expressed by

$$k E_{\parallel} = k-1 E_{\parallel} R_{\parallel} R_{\parallel} R_{\parallel} + k-1 E_{\perp} R_{\perp} R_{\perp} R_{\parallel} \quad (9)$$

$$k E_{\perp} = k-1 E_{\parallel} R_{\parallel} R_{\parallel} R_{\perp} + k-1 E_{\perp} R_{\perp} R_{\perp} R_{\perp} \quad (10)$$

where  ${}_0 E_{\parallel} = E_{\parallel t}$  and  ${}_0 E_{\perp} = E_{\perp t}$ . The quantities  ${}_k E_{\parallel}$  and  ${}_k E_{\perp}$  for  $k = n$ , represent the field of the  $n$ -hop ray uncorrected for path length. The fields are then corrected for path length by

$$E_{\parallel}^{(n)} = {}_n E_{\parallel} \frac{1}{R_n} \cdot \exp(j \angle T_n) \quad (11)$$

$$E_{\perp}^{(n)} = {}_n E_{\perp} \frac{1}{R_n} \cdot \exp(j \angle T_n) \quad (12)$$

where  $E_{\parallel}^{(n)}$ ,  $E_{\perp}^{(n)}$ ,  $R_n$  and  $\angle T_n$  are the parallel polarized component, perpendicular polarized component, propagation distance and phase of

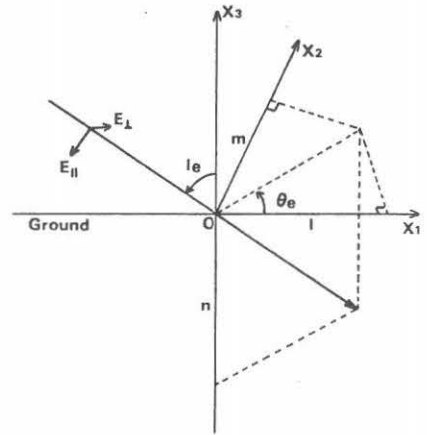


Fig.2 The coordinate system. The  $x_1$ - $x_3$  plane is the plane of incidence.

the  $n$ th-order ray, respectively.

The series of rays arriving at a different angle  $I_n$ , each containing a parallel and a perpendicular component of electric field, have components in all three coordinate directions. So, we can decompose the wave into these components:

$$E_{x1} = \sum_n E_{||}^{(n)} \cos I_n = |E_{x1}| \exp(j\phi_1) \quad (13)$$

$$E_{x2} = \sum_n E_{\perp}^{(n)} = |E_{x2}| \exp(j\phi_2) \quad (14)$$

$$E_{x3} = \sum_n E_{||}^{(n)} \sin I_n = |E_{x3}| \exp(j\phi_3) \quad (15)$$

The coordinate system is shown in Fig.2. The  $x_1$ - $x_3$  plane is the plane of incidence. Since the three axial components of field have independent phases and amplitudes, the figure that the total field vector describes is an ellipse. We can determine the orientation of the plane of this ellipse, and the incident and azimuthal angles of the normal of this plane is given by,

$$\theta_e = \tan^{-1}(m/\ell) \quad , \quad I_e = \tan^{-1}\left(-\frac{\sqrt{\ell^2 + m^2}}{n}\right) \quad (16)$$

where

$$\ell^2 = \sin^2(\phi_2 - \phi_3) / [\sin^2(\phi_2 - \phi_3) + (|E_{x1}|/|E_{x3}|)^2 \cdot \sin^2(\phi_1 - \phi_2) + (|E_{x1}|/|E_{x2}|)^2 \cdot \sin^2(\phi_3 - \phi_1)] \quad (17)$$

$$m = \ell \cdot |E_{x1}| \cdot \sin(\phi_3 - \phi_1) / [|E_{x2}| \sin(\phi_2 - \phi_1)] \quad (18)$$

$$n = \ell \cdot |E_{x1}| \cdot \sin(\phi_1 - \phi_2) / [|E_{x3}| \sin(\phi_2 - \phi_3)] \quad (19)$$

The errors in incident and azimuthal angles caused by multi-rays are defined by

$$\Delta I = I_e - I_0 \quad , \quad \Delta \theta = \theta_e \quad (20)$$

where the angle  $I_0$  is the incident angle of a direct ray ( $n=0$ ). Then the polarization of the total field is given by

$$\begin{aligned}
 P &= E_{\perp} / E_{\parallel} \\
 &= (E_{x1} \sin\theta_e - E_{x2} \cos\theta_e) / [-(E_{x1} \cos\theta_e + E_{x2} \sin\theta_e) \cos I_e \\
 &\quad + E_{x3} \sin I_e] \tag{21}
 \end{aligned}$$

The polarization is right handed circular when  $|P|=1$  and  $\arg(P)=-90^\circ$ .

#### 4. Computational results

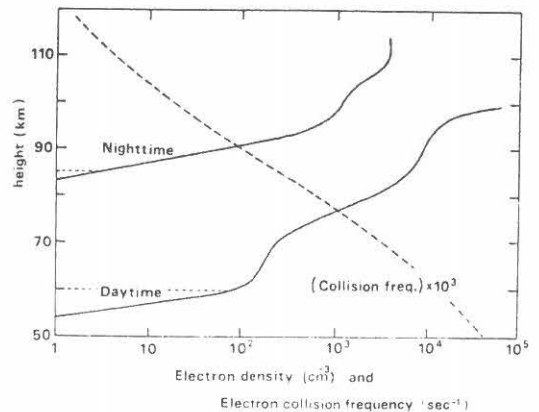
##### 4.1. Ionospheric model

The calculations are carried out for ionospheric parameters given in Table 1. The gyro-frequency and geomagnetic dip angle correspond to the geomagnetic latitude of  $34.5^\circ$  North referring to our Moshiri observatory. In the computation, we choose a specific frequency of 5.6kHz for the wave frequency because our DF measurements have been made at this frequency. The ionospheric models at night and by day are given in Fig.3.

Table 1. Ionospheric parameters.

|                            |  |
|----------------------------|--|
| Gyro-frequency             | 1161.16kHz                                 |
| Magnetic dip angle         | $52.88^\circ$                              |
| Ionospheric model          | daytime, nighttime                         |
| Reflection height( $h_r$ ) | 60km (for daytime)<br>85km (for nighttime) |

Fig.3 The daytime and nighttime ionospheric models used in the computations. The lower part of the profiles when we expect the partial reflection can be approximated by exponential models.

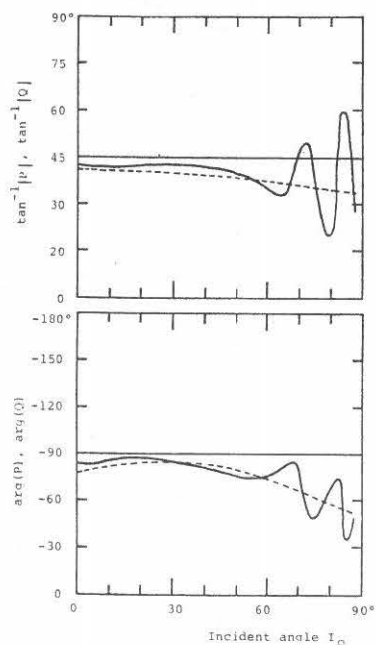




#### 4.2. The characteristics of resultant polarization

Figures 4 and 5 are the results of polarization. The broken lines indicate the limiting polarization for a direct ray ( $Q$  in Eq.(5)) and the full lines refer to the polarization of the total field ( $P$  in Eq.(21)). The calculation is made for the nighttime ionospheric model. Fig.4 shows how the limiting polarization  $Q$  varies with incident angle  $I_0$  of a direct ray and also how the polarization  $P$  changes with incident angle  $I_0$  of a corresponding direct ray, in the case of South to North propagation in the Northern hemisphere ( $\theta_0=180^\circ$ ). For the incident angle  $I_0$  less than  $60^\circ$ , the polarization of the total field can be considered to be nearly circular, and also it is not so much different from the limiting polarization for the direct ray. This indicates that the contribution of a direct ray is considerably dominant and the higher order multi-rays ( $n=1,2,\dots$ ) are not so influential on the polarization. With the increase of  $I_0$  above  $60^\circ$ , the polarization ( $P$ ) is found to oscillate around the broken line of the limiting polarization of a direct ray. The contribution to the total field from the multi-rays is enhanced compared to that of a direct ray for the larger incident angle  $I_0$  on the following reasons. The first is that the ratio of the path length of successive order rays decrease with the increase of the ground distance  $D$ , and the other is the relative decrease of the contribution of an input direct ray because the larger the incident angle the smaller the transmission coefficient.

Fig.4 Variation of polarization with incident angle  $I_0$  for nighttime ionospheric model. The broken and full lines indicate the limiting polarization ( $Q$ ) for a direct ray and the polarization ( $P$ ) of the total field, respectively.



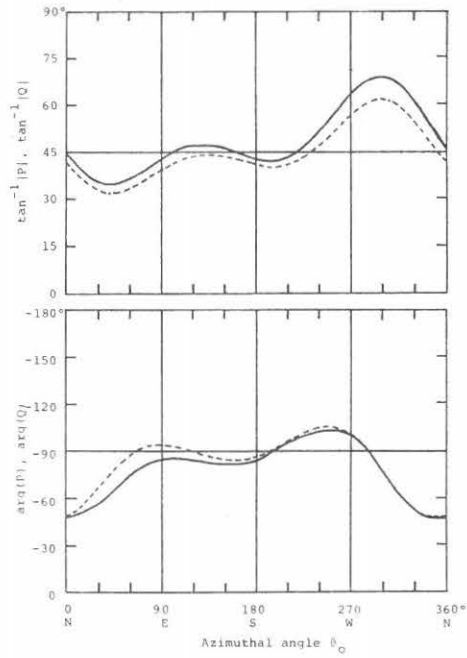


Fig.5(a) Azimuthal dependence in the case of  $I_0=30^\circ$ .

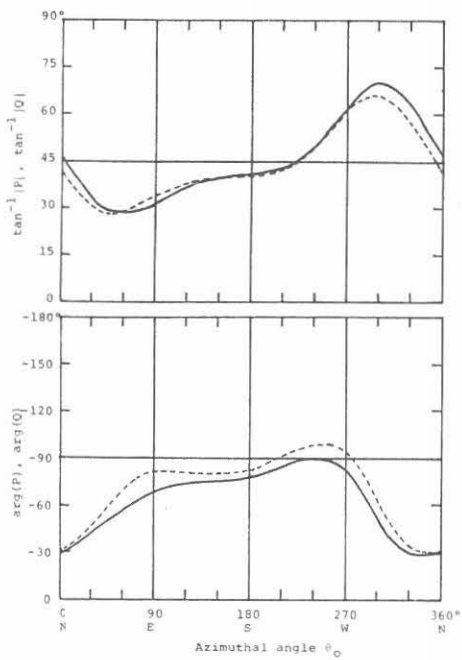


Fig.5(b) Azimuthal dependence in the case of  $I_0=45^\circ$ .

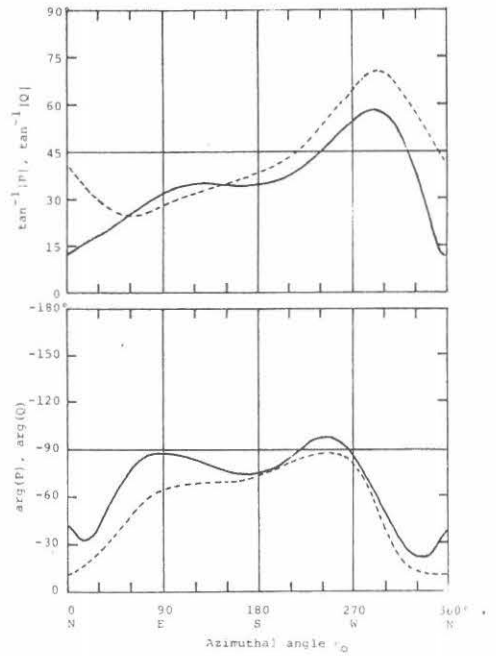


Fig.5(c) Azimuthal dependence in the case of  $I_0=60^\circ$ .

Fig.5 Azimuthal dependence of polarization for nighttime model.

Figs.5 show the azimuthal dependence of the polarizations Q and P with three different direct ray angles ( $I_o$ ) of  $30^\circ$  (Fig.5(a)),  $45^\circ$  (Fig.5(b)) and  $60^\circ$  (Fig.5(c)).  $\theta_o=0^\circ$  indicates North to South,  $\theta_o=90^\circ$  East to West,  $\theta_o=180^\circ$  South to North and  $\theta_o=270^\circ$  West to East propagation in the Northern hemisphere. The difference of the polarization of a direct ray and of the total field is already found to be relatively small for  $I_o$  less than  $60^\circ$  for a specific direction ( $\theta_o=180^\circ$ ), as shown in Fig.4, and this tendency is confirmed to be valid for other azimuthal directions in the case of  $I_o$  less than  $60^\circ$  (see Figs.5(a) and 5(b)). As can be expected from the variation in Fig.4 we understand that there is a significant difference between the polarization of the total field and a direct ray for  $I_o$  greater than  $60^\circ$ . Fig.5(c) indicates that the difference shows a maximum at  $\theta_o=0$ , or North to South propagation, and so the influence of multi-rays is maximized in this propagating direction. The polarization P is found to be closer to circular for the azimuth  $\theta_o$  from  $90^\circ$  to  $270^\circ$ , while it is closer to linear for other azimuthal directions. The most circular polarization is seen at  $\theta_o \approx 225^\circ$ , and the most linear polarization is found at  $\theta_o \approx 330^\circ$ .

Similar computational results for daytime ionospheric model are given in Figs.6 and 7. Fig.6 shows that for the smaller incident angle  $I_o < 60^\circ$ , the wave polarization (P) seems to be closer to circular than in the case of nighttime ionosphere. It is likely from Fig.7 that the polarization does not show a significant variation with azimuth compared with that at night. This is apparently due to that the absorption due to the collision in the lower ionosphere is dominant over the effect of Earth's magnetic field during daytime.

#### 4.3. The error in the measurement of incident and azimuthal angles

Figures 8 and 9 show the results of the error in incident and azimuthal angles due to the effect of multi-rays for the nighttime model. Fig.8 shows the variation of the error ( $\Delta I$ ) in incident angle and ( $\Delta \theta$ ) in azimuthal angle with incident angle  $I_o$  in the case of South to North propagation ( $\theta_o=180^\circ$ ). The errors of  $\Delta I$  and  $\Delta \theta$  are relatively small for the incident angle  $I_o$  less than  $60^\circ$  such that  $\Delta I$  is less than  $6^\circ$  and  $\Delta \theta$  less than  $10^\circ$ , respectively. But, with the increase of incident angle larger than  $60^\circ$ , the errors of  $\Delta I$  and  $\Delta \theta$  are seen to oscillate with large amplitudes and  $\Delta I$  varies from  $-15^\circ$  to  $19^\circ$  and  $\Delta \theta$  from  $-18^\circ$  to  $23^\circ$ , respectively. Fig.9 illustrates the azimuthal dependence of the errors  $\Delta I$  and  $\Delta \theta$  for three specific values of  $I_o =$

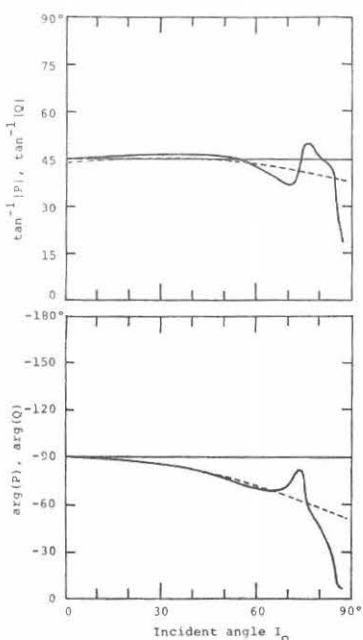


Fig.6 Variation of polarization with incident angle  $I_0$  for day-time ionospheric model.

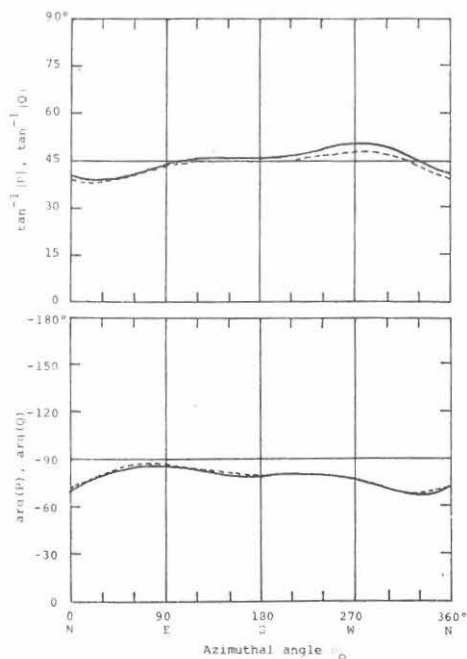


Fig.7 Azimuthal dependence of polarization for daytime model in the case of  $I_0=45^\circ$ .

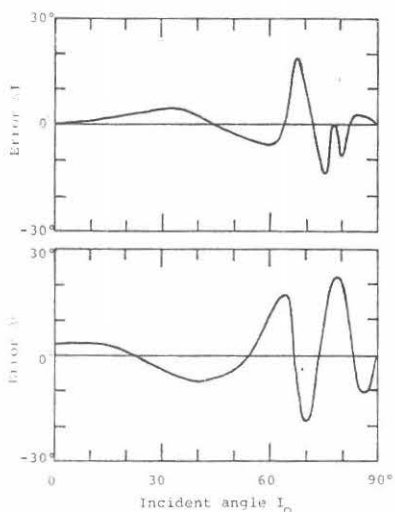


Fig.8 The errors of  $\Delta I$  and  $\Delta\theta$  as a function of incident angle  $I_0$  in the case of the South to North propagation for the nighttime model.

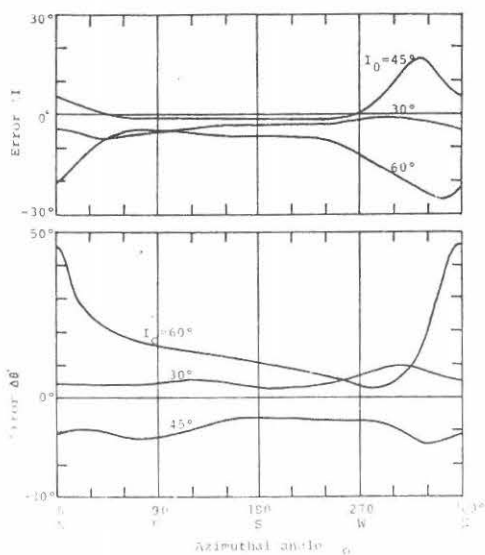


Fig.9 Azimuthal dependence of the errors of  $I$  and  $\Delta\theta$  in the cases of  $I_0=30^\circ, 45^\circ$  and  $60^\circ$  for nighttime model.

30°, 45° and 60°. It seems that the azimuthal dependence is not so much in the case of  $I_0=30^\circ$ , whereas the errors of  $\Delta I$  and  $\Delta\theta$  for  $I_0=60^\circ$  exhibit remarkable azimuthal dependence such that the errors  $\Delta\theta$  varies from 3° to 46° over the whole azimuth. The error is maximized in the North to South propagating direction ( $\theta_0=0$ ), and this is due to the fact that the effect of multi-rays is most effective in this direction as mentioned in the previous section.

The corresponding computational results of the errors  $\Delta I$  and  $\Delta\theta$

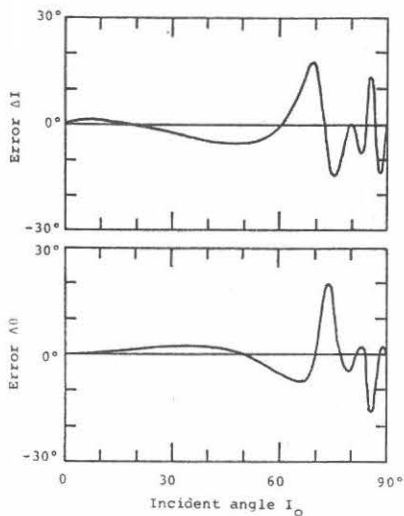


Fig.10 The errors of  $\Delta I$  and  $\Delta\theta$  as a function of incident angle  $I_0$  for daytime model.

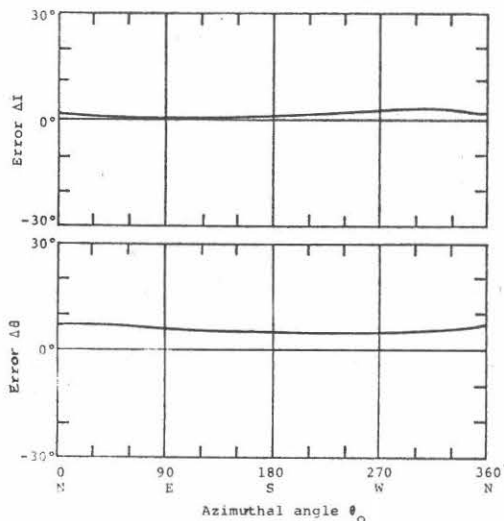
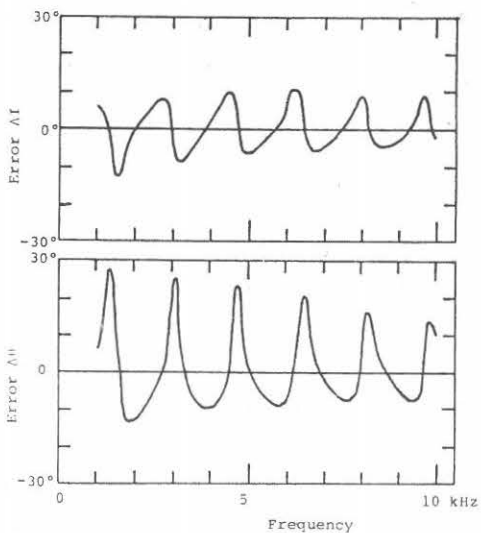


Fig.11 Azimuthal dependence of the errors  $\Delta I$  and  $\Delta\theta$  in the case of  $I_0=45^\circ$  for daytime.

Fig.12 The frequency dependence of the errors  $\Delta I$  and  $\Delta\theta$  in the case of  $I_0=45^\circ, \theta_0=180^\circ$  for nighttime model.



for the daytime ionosphere are given in Figs.10 and 11. When the incident angle is less than  $60^\circ$ , both of the errors  $\Delta I$  and  $\Delta \theta$  are smaller than  $5^\circ$ . And we find insignificant dependence of the errors with azimuthal direction.

From these results we may conclude that, under the normal situation of the field analysis method DF measurements, the errors of  $\Delta I$  and  $\Delta \theta$  owing to the effect of multi-rays are found to be less than  $10^\circ$  and  $15^\circ$  for nighttime, and less than  $5^\circ$  and  $10^\circ$  for daytime, respectively. In general, the error by day is smaller than that at night because the reflection coefficients of the daytime ionosphere are nearly one half of those at night, resulting in the reduced effect of multi-rays by day. Furthermore, there is a little azimuthal dependence by day. So, we have to pay significant attention to the effect of multi-rays in interpreting the DF data at night.

Additionally, we have calculated the frequency dependence of the errors for a specific combination of  $I_o$  and  $\theta_o$ . The result is shown in Fig.12. The errors  $\Delta I$  and  $\Delta \theta$  is found to show a regular oscillation with large amplitudes, and so their average value over a wide range in frequency tends to zero, as was first pointed out by Cray (1961). And this principle was used by Cousins (1973) and Leavitt et al. (1978) to reduce the polarization errors caused by multi-rays.

## 5. Discussion and future problems

One of the most important results emerged from the present calculations is that the polarization of the resultant wave field as the superposition of multi-rays from a point source is found to be very close to the limiting polarization of a corresponding direct ray for the incident angle  $I_o$  less than  $60^\circ$ , and the polarization is nearly circular in that range. The recent observation by Okada et al. (1977), has yielded that some whistlers have a polarization close to circular, but the polarization of a considerable number of whistlers is greatly different from circular even for the overhead exit. Such a great difference of polarization from circular cannot be explained only by the effect of multi-rays discussed in the present paper. This discrepancy may be resulted from the inaccuracy of the model of calculation used in the present paper. The most probable possibility of the discrepancy may be related to the assumption of the emergence of waves from a point source, and we should consider a more general case in

which the emergence region cannot be considered a point source, but it has a significant extent indicating the integral of point sources. Then the polarization can be determined by the superposition of multiple direct rays emerging from various points over the significantly spread region. The calculation in this direction such as done by Tanaka et al. (1976) is being carried out. However, when the observed whistler has a polarization very close to circular, the emergence region for the relevant whistler can be regarded as a point source, as is inferred from the present paper, and the results in the present paper are still very useful. The polarization is not used as an informative quantity so often, but it seems likely that the polarization may provide us with the important information on the extent of emergence region of whistlers.

Based on the results in the present paper, suggestions in interpreting the field analysis DF data are summarized as follows.

(1) By using the observed whistler polarization, we have to group the whistlers into those with a nearly circular polarization and those with a polarization considerably different from circular.

(2) For whistlers with a nearly circular polarization, the emergence region at the base of the ionosphere can be regarded as "a point source", and also the error in the measurement of arrival direction (incident and azimuthal angles) is relatively small, of the order of  $10^\circ$ . In this case, the frequency dependence of the exit points (Okada et al., 1978) will be useful for the investigation of the propagation mechanism of low-latitude whistlers (Hayakawa and Tanaka, 1978).

(3) When the observed whistler polarization departs from circular, the emergence region at the ionospheric base seems to have a significant extent. The polarization is determined by the superposition of multiple direct rays from various points in the spread emergence region, and we expect a great error in the measurement of arrival angles, probably greater than  $10^\circ$ .

(4) It may be possible that we can deduce or guess the extent of emergence region and mechanism of transmission by making use of the polarization data.

### Acknowledgement

The authors wish to express their sincere thanks to Prof. I. Kimura, Dept. of Electrical Engineering, Kyoto University and Prof. J. Ohtsu of their institute for their useful criticism and suggestion.

### References

- Bullough K. and J.L. Sagredo : VLF goniometer observations at Halley Halley Bay, Antarctica-I. The equipment and the measurement of signal bearing. *Planet. Space Sci.*, 21, 899 (1973).
- Corcuff Y. : Probing the plasmopause by whistlers. *Ann. Géophys.*, 26, 363 (1975).
- Cousins M.D. : Direction finding on whistlers and related VLF signals. SEL-72-013. Radioscience Lab., Stanford Univ., CA. (1972).
- Crary J.H. : The effect of the earth-ionosphere waveguide on whistlers. Tech. Rept. No.9. Radioscience Lab., Stanford Univ., CA. (1961).
- Hayakawa M. and S. Shimakura : On the mechanism of reflection of ELF-LF radio waves from the lower ionosphere. *Trans. IECE*, E61, 15 (1978).
- Hayakawa M. and Y. Tanaka : On the propagation of low-latitude whistlers. *Rev. Geophys. Space Phys.*, 16, 111 (1978).
- Leavitt M.K., Carpenter D.L., Seely N.T., Radden R.R. and J.H. Doolittle : Initial result from a tracking receiver direction finder for whistler mode signals. *J. Geophys. Res.*, 83, 1601 (1978).
- Okada T., Iwai A. and M. Hayakawa : The measurement of incident and azimuthal angles and the polarization of whistlers at low latitudes. *Planet. Space Sci.*, 25, 233 (1977).
- Okada T., Moriyama S. and A. Iwai : Development of a two-frequency direction finder for whistlers. *Trans. IECE*, 61, 993 (1978).
- Pitteway M.L.V. : The numerical calculation of wave-fields, reflection coefficients and polarization of long radio waves in the ionosphere. *Phil. Trans. Roy. Soc.*, A257, 219 (1965).
- Pitteway M.L.V. and J.L. Jespersen : A numerical study of the excitation, internal reflection and polarization of whistler waves in the lower ionosphere. *J. Atmosph. Terr. Phys.*, 28, 17 (1966).



- Rycroft M.J., Jarvis M.J. and H.J. Strangeways : Determination by triangulation of the regions where whistlers emerge from the ionosphere. ESRO Special Publ., No.107, P.225 (1974).
- Tanaka Y. : VLF hiss observed at Showa Station, Antarctica. 1. Observation of VLF hiss. Proc. Res. Inst. Atmos. Nagoya Univ.,19,33 (1972).
- Tanaka Y., Hayakawa M. and M.Nishino : Study of auroral VLF hiss observed at Syowa Station, Antarctica, Mem. Natl. Inst. Polar Res. Tokyo, Series A, A13 (1976).
- Tsuruda K. and K.Hayashi : Direction finding technique for elliptically polarized VLF electromagnetic waves and its application to the low-latitude whistlers. J. Atmosph. Terr. Phys.,37,1193 (1975).

